Computational and Theoretical Chemistry 1015 (2013) 15–20

Contents lists available at SciVerse ScienceDirect

Computational and Theoretical Chemistry

journal homepage: www.elsevier.com/locate/comptc

Xenon oxides, sulfides, and oxysulfides. A theoretical ab initio investigation

Aristotle Papakondylis *

Department of Chemistry, Laboratory of Physical Chemistry, National and Kapodistrian University of Athens, Panepistimiopolis, Zografou, Athens 157 71, Greece

ARTICLE INFO

Article history:
Received 19 February 2013
Received in revised form 20 March 2013
Accepted 31 March 2013
Available online 17 April 2013

Keywords:
Xenon
Oxides
Sulfides
Oxysulfides
Ab initio

ABSTRACT

We present ab initio RCCSD(T)/aug-cc-pV5Z results on the closed shell systems XeO_nS_m with n, m = 0, 1, 2, 3, 4 and $1 \leqslant n + m \leqslant 4$, a total of 14 molecules. Geometrical parameters, binding and atomization energies, dipole moments and harmonic frequencies are provided for all title species. Moreover, the bonding mechanisms, as well as, the possibility of isolating some of them are discussed.

1. Introduction

Xenon is, perhaps, the most reactive element among rare gases due to the effective shielding of its valence electrons by the inner ones. Xenon oxides, fluorides and oxyfluorides were synthesized in the early sixties [1–4]. The preparations of XeO_3 [5] and of XeO_4 [6,7] were reported in 1963 and 1964, respectively. XeO_3 forms non-volatile colorless crystals, while XeO_4 is a yellow solid at low temperature and unstable at room conditions. Both are highly explosive. Several experimental studies were carried out in order to determine the structure [8,9], vibrational spectra [10–12], and enthalpies of formation [13–15] of these compounds.

Bartlett and Rao [16], in 1963, speculated the discovery of xenon dioxide in the experimentally obtained $Xe(OH)_4$ (or $XeO_2{\cdot}2H_2O$) white solid which also was explosive above ~30 °C. Very recently, Brock and Schrobilgen [17] announced the synthesis of a bright yellow solid with the XeO_2 stoechiometry. They used Raman spectroscopy and isotopic enrichment techniques to show that this solid consisted of "polymerized" XeO_2. However, the observation of molecular XeO_2 still remains uncertain.

Now, concerning the XeO diatomic, a green emission band system was observed [18–20], which was attributed, to the xenon monoxide $2^1\Sigma^+ \rightarrow 1^1\Sigma^+$ transition. Both states involved in this transition are excited states of the system. As shown by Dunning and Hay [21], in the first theoretical work on rare gas oxides, the XeO ground state is of $^3\Pi$ symmetry. This state together with a $^3\Sigma^-$ state, stem from the $Xe(^1S) + O(^3P)$ asymptotic channel. They are of repulsive character and cross the potential energy curve (PEC) of the first bound $^1\Sigma^+$ state, emerging from the $Xe(^1S) + O(^1D)$ asymptote. In 1980 Langhoff [22] studied the spin–orbit coupling between $1^1\Sigma^+$ and the $^3\Sigma^-$, 3Π states for all rare gas monoxides in order to determine the efficiency of the collisional quenching $Rg + O(^1D) \rightarrow Rg + O(^3P)$. A more thorough study of the low-lying electronic states of XeO and XeS was reported by Yamanichi et al. [23]. These workers used the MRSDCI methodology coupled with double-ζ quality basis sets to construct PEC's of nine electronic states. For the $1^1\Sigma^+$ state of XeO they computed a binding energy of 0.77 eV.

The first theoretical investigation concerning XeO_n systems, with n = 2, 3, 4, was published in 2000 by Pyykkö and Tamm [24]. These authors focused mainly on the possibility of isolation of XeO_2. They employed the CCSD(T) method in conjunction with triple-ζ bases and obtained results for XeO_3 and XeO_4 in relatively good agreement with existing experimental data. Concerning XeO_2, they computed a slightly negative atomization energy but they claimed that XeO_2 might be observed at low temperature due to the kinetic stability brought about by a barrier of, at most, 115 kJ/mol.

In the same year, Ball [25] examined theoretically the possibility of stable binary and trinary xenon–oxygen–sulfur compounds. He performed HF, DFT, and MP2 calculations on the series XeO_3, XeO_2S, $XeOS_2$, and XeS_3. For all species he found local minima with real harmonic frequencies and he also computed the corresponding enthalpies of formation. It must be noted that none of the xenon sulfides or the mixed Xe–O–S systems has been, so far,

* Tel.: +30 2107274565; fax: +30 2107274752.
E-mail address: papakondylis@chem.uoa.gr

2210-271X/$ - see front matter © 2013 Elsevier B.V. All rights reserved.
http://dx.doi.org/10.1016/j.comptc.2013.03.030

synthesized. The only xenon sulfide detected was XeS. Its near-IR emission spectrum was recorded in rare-gas matrices by Taylor and Walker [26], in 1979. As in the case of XeO, the luminescence observed, was attributed to the $2^1\Sigma^+ \rightarrow 1^1\Sigma^+$ transition. Yamanichi et al. [23] showed theoretically that XeO and XeS have very similar PEC profiles and the binding energy of the $1^1\Sigma^+$ state of XeS is less than half that of XeO.

Now, in the present paper we carry out a systematic high level ab initio study of the lowest closed shell state of all possible XeO_nS_m species, i.e. with n, $m = 0, 1, 2, 3, 4$ and $1 \leqslant n + m \leqslant 4$, a total of 14 different molecular systems. Our goal was to provide very accurate theoretical results concerning the structural properties and energetics of these systems. We present geometrical parameters, binding and atomization energies, dipole moments and harmonic frequencies for all species studied. Moreover, we discuss on their bonding mechanism and, also, on the possibility of isolating some of them.

2. Computational outline

Through all calculations we employed the restricted coupled-cluster singles and doubles with a perturbation treatment of triples, RCCSD(T), methodology.

For the Xe atom we used the augmented quintuple-ζ correlation consistent small core pseudopotential basis set of Peterson et al. [27], aug-cc-pV5Z-PP, contracted as (17s14p14d4f3g2h) → [8s8p6d4f3g2h]. This basis set replaces the [Ar]$3d^{10}$ core of Xe with a relativistic potential and comprises 139 spherical Gaussians. The corresponding aug-cc-pV5Z bases of Dunning were, also, used for oxygen [28] and sulfur [29].

We have correlated at the RCCSD(T) level all valence electrons, namely Xe($5s^25p^6$) + O ($2s^22p^4$) or S($3s^23p^4$). This computational scheme yields the following absolute atomic energies: Xe(^{1}S) −328.49903 E_h, O(^{3}P) −75.00041 E_h, O(^{1}D) −74.92095 E_h, S(^{3}P) −397.67143 E_h, S(^{1}D) −397.62425 E_h. Thus, the O(^{1}D) → O(^{3}P) and S(^{1}D) → S(^{3}P) energy separations were found 2.162 and 1.284 eV, respectively, slightly greater than the experimental [30] 1.958 and 1.121 eV values. These differences are due to our single reference description of the ^{1}D state. All D_0 values reported here were corrected for this small asymptotic error.

The basis set superposition errors calculated by the counterpoise method, never exceeded the 4×10^{-4} E_h value.

Harmonic frequencies were calculated using the corresponding aug-cc-pVTZ-PP [27] for the Xe atom and aug-cc-pVTZ [28,29] for O and S, in order to make tractable the time consuming numerical Hessian computations. For Xe the average isotopic atomic mass was used.

All dipole moments were evaluated through the finite field approach by applying a 5×10^{-6} a.u. electric field.

In the case of the XeO and XeS diatomics, we performed also MRCI calculations which consisted of single and double replacements out of a CASSCF space defined by allotting 10 [O or S($2p^4$) + -Xe($5p^6$)] electrons to 10 orbitals. The Xe $5s^2$ and O or S $2s^2$ electrons were correlated at the CISD level. The MRCI spaces ranged from 1.6×10^9 to 3.1×10^9 configuration functions (CF) internally contracted to $\sim 15 \times 10^6$–27×10^6 CFs. Size non-extensivity errors were corrected using multireference Davidson correction (MRCI + Q).

The MOLPRO 2010.1 code [31] was used through all our calculations.

3. Results and discussion

3.1. Oxides

Table 1 summarizes our results concerning the lowest closed singlet state of each of the XeO($^1\Sigma^+$), XeO_2($^1A_1$), XeO_3($^1A_1$), and XeO_4($^1A_1$) systems. For the XeO species we also present, in Fig. 1, potential energy curves of the lowest three electronic states, $^3\Pi$, $^3\Sigma^-$, and $^1\Sigma^+$. As we can see from this figure, the first two states, stemming from the ground state atomic asymptote, are of repulsive nature with only very weak van der Waals interactions at 3.596 Å (D_e = 125 cm^{-1}) and 4.150 Å (D_e = 64 cm^{-1}), respectively. The first bound electronic $^1\Sigma^+$ state correlates adiabatically to the Xe(^{1}S) + O(^{1}D) channel and crosses the $^3\Pi$ and $^3\Sigma^-$ PEC's at r(Xe−O) = 2.188 and 2.401 Å, respectively. From Table 1 we have for this state: r_e = 1.923 Å, D_0 = 33.7 kcal/mol, and ω_e = 594 cm^{-1}. Our numbers are in serious disagreement with the corresponding r_e = 2.06 Å, D_0 = 17.8 kcal/mol, and ω_e = 472 cm^{-1} values by Yamanishi et al. [23]. This discrepancy is due to the fact that the basis sets used by these authors (double-ζ and large core for Xe) are rather poor. We were able to reproduce their results with the same basis sets. The atomization XeO($^1\Sigma^+$) → Xe(^{1}S) + O(^{3}P) process is exothermic by 10.6 kcal/mol. This process contributes to the quenching mechanism Xe + O(^{1}D) → XeO($^1\Sigma^+$) → Xe + O(^{3}P) and is regulated by the efficiency of the spin–orbit coupling to generate the necessary intersystem crossing. The interaction Xe(^{1}S) + O(^{1}D) can be depicted by the valence bond-Lewis (vbL) diagram of Scheme 1.

In this scheme, only the first term of the $|^1D; M_L = 0\rangle = \frac{1}{\sqrt{6}}(2|p_x^2p_y^2| - |p_x^2p_z^2| - |p_y^2p_z^2|)$ atomic wavefunction of oxygen is shown. As we can see, an electron pair is transferred from Xe towards the empty p_z orbital of O to form a dative bond. This mechanism does not imply any electron recoupling and this

Table 1
Energies E (E_h), geometrical parameters (Å, deg), binding energies D_0 (kcal/mol), atomization energies ΔH_{atom} (kcal/mol), dipole moments μ (D), net Mulliken charges q (e), and harmonic frequencies ω_e (cm^{-1}) of the lowest closed singlet state of XeO_n, n = 1–4.[a]

Species	$-E$	r(Xe–O)	∠O–Xe–O	D_0[b]	ΔH_{atom}[c]	μ	q_{Xe}	ω_e
XeO($^1\Sigma^+$)	403.482597	1.923	–	33.7	−10.6	3.8	+0.87	594
XeO_2($^1A_1$)	478.506480	1.840	112.1	92.2	1.9	3.9	+1.96	a_1 198, a_1 681, b_2 728
XeO_3($^1A_1$) (expt)	553.579031	1.779 (1.760)[d]	106.8 (103)[d]	180.2	44.7 (52.5 ± 12)[e]	3.5	+3.12	e 262, a_1 304, a_1 777, e 852 (e 317, a_1 344, a_1 780, e 833)[f]
XeO_4($^1A_1$) (expt)	628.624297	1.757 (1.736)[g]	109.47 (109.47)[g]	251.4	70.7 (84.4)[h]	0.0 (0.0)	+4.00	e 253, t_2 304, a_1 774, t_2 868 (e 267, t_2 306, a_1 776, t_2 879)[i]

[a] Net Mulliken charges are from HF calculations, harmonic frequencies are obtained at the RCCSD(T)/aug-cc-pVTZ level. All other numbers are at the RCCSD(T)/aug-cc-pV5Z level.
[b] With respect to Xe(^{1}S) + nO(^{1}D).
[c] With respect to Xe(^{1}S) + nO(^{3}P).
[d] Solid state crystallographic average values, Ref. [8].
[e] Thermochemical data assuming a sublimation enthalpy 30 ± 10 kcal/mol, Ref. [13].
[f] Raman spectrum of aqueous solution, Ref. [10].
[g] Ref. [9].
[h] Enthalpy of formation from thermochemical studies, Ref. [14], and assuming a 119 kcal/mol binding energy for O_2.
[i] Gas phase, Ref. [12].

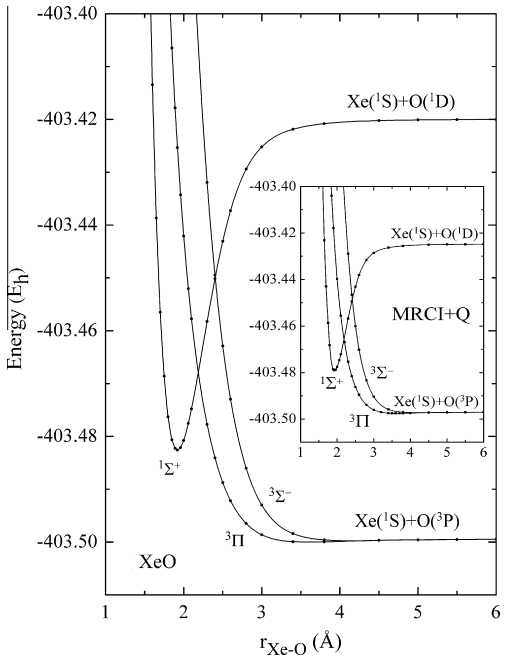

Fig. 1. Potential energy curves of the low-lying $^3\Pi$, $^3\Sigma^-$, and $^1\Sigma^+$ electronic states of XeO at the RCCSD(T)/aug-cc-pV5Z and MRCI + Q/aug-cc-pV5Z (inset) levels of theory.

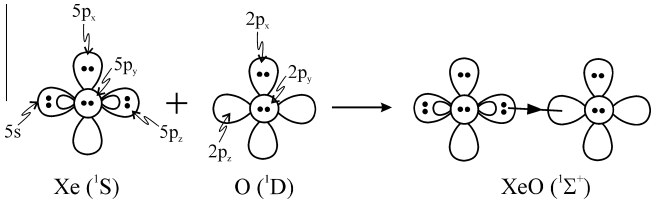

Scheme 1.

is why we were able to construct the corresponding PEC, Fig. 1, with the single referenced RCCSD(T) method.

In order to confirm this assumption we performed CASSCF/MRCI calculations (see Section 2). The potential energy curves obtained at the MRCI + Q level are shown in the inset of Fig. 1. As we can see, these curves are surprisingly similar to the ones constructed through the RCCSD(T) methodology. The results obtained are almost the same as the RCCSD(T) ones, Table 1. For instance at the MRCI + Q level we found for the $^1\Sigma^+$ state r_e(XeO) = 1.927 Å, D_0 = 34.1 kcal/mol, ΔH_{atom} = −10.7 kcal/mol, μ = 3.7 D, and ω_e = 585 cm^{-1}. For this state the leading MRCI configuration at equilibrium is the HF wavefunction $|1\sigma^2 2\sigma^2 3\sigma^2 1\pi^4 2\pi^4\rangle$ (where only valence orbitals are counted) with a coefficient 0.97. This clearly denotes a single reference character which persists all along the potential energy curve. Analyzing the 3σ doubly occupied MO we see that it represents a bonding interaction between Xe(5p$_z$) and O(2p$_z$) AO's. As a result, the population analysis (using the MRCI natural orbitals) shows that an important fraction of the Xe(5p$_z$) electron pair is shared with O(2p$_z$), in accord with the mechanism of Scheme 1. The bond gains a marked ionic character which is reflected in the corresponding dipole moment which was found 3.8 D, a rather large value.

The following spectroscopic constants were calculated for XeO($1^1\Sigma^+$) by numerically solving the rovibrational Schrödinger equation: ω_e = 594 cm^{-1}, $\omega_e x_e$ = 5.2 cm^{-1}, a_e = 2.8 × 10^{-3} cm^{-1}, and $\bar{D}_e$ = 2.8 × 10^{-7} cm^{-1}.

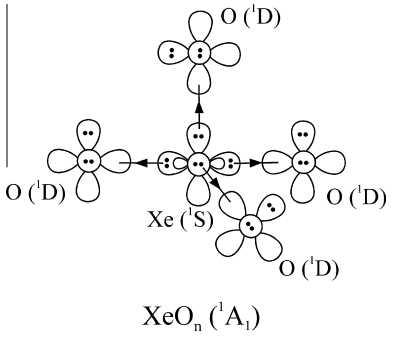

Scheme 2.

We move now to the polyatomic xenon oxides, XeO$_n$, n = 2, 3, 4. The corresponding molecular symmetries are C_{2v} (n = 2), C_{3v} (n = 3), and T_d (n = 4). We are always interested in the lowest $^1A_1$ closed singlet of each of those systems. The bonding mechanism can only be the same as in the case of XeO($1^1\Sigma^+$), i.e. Xe(^{1}S) + nO(^{1}D) → XeO$_n$ (^{1}A$_1$). This is confirmed by the corresponding Mulliken populations and is illustrated by Scheme 2. Here again, xenon electron pairs move toward the empty p orbital of each O(^{1}D) entity, forming dative bonds. In this way, 2, 3, or 4 oxygen atoms can be linked to the central Xe atom as shown by the vbL diagram of Scheme 2.

Binding energies D_0 (with respect to Xe(^{1}S) + nO(^{1}D)), as well as, atomization energies ΔH_{atom} (with respect to Xe(^{1}S) + nO(^{3}P)) are reported in Table 1. All values include zero point energy (ZPE) corrections. First, we see that in all cases we have important D_0 values. Second, all three XeO$_n$ species are bound with respect to the atomic ground state asymptote. We observe a monotonic increase of the mean Xe–O binding energy (D_0/n) as the number of oxygen atoms increases, namely (in kcal/mol), 33.7 (n = 1) → 46.1 (n = 2) → 60.1 (n = 3) → 62.9 (n = 4). This is also reflected in the fact that bond-lengths decrease with increasing number of oxygen atoms. One could talk about a synergistic effect due to the augmentation of the Xe positive charge with each oxygen added, Table 1, which leads to a more pronounced ionic character of each Xe–O bond.

For the XeO$_2$ species we have computed a slightly positive atomization energy ΔH_{atom} = 1.9 kcal/mol. This is an improvement over the previous theoretical value ΔH_{atom} = −3.6 kcal/mol reported by Pyykkö and Tamm [24]. Thus, our result somewhat reinforces the claim of these authors that XeO$_2$ could be detected under proper conditions.

Now, the atomization energies of XeO$_3$ and XeO$_4$ were found 44.7 and 70.7 kcal/mol, respectively, greater by 9.6 and 14.3 kcal/mol, than the corresponding values of Pyykkö and Tamm. The experimental ΔH_{atom} = 84 kcal/mol, deduced from thermochemical data of Ref. [10] for XeO$_4$, is deemed rather excessive.

Concerning the individual Xe–O bond strengths the following numbers were computed at the RCCSD(T)/aug-cc-pV5Z level:

$$XeO_4(^1A_1) \rightarrow XeO_3(^1A_1) + O(^3P) \quad 26 \text{ kcal/mol}$$

$$XeO_3(^1A_1) \rightarrow XeO_2(^1A_1) + O(^3P) \quad 42.8 \text{ kcal/mol}$$

$$XeO_2(^1A_1) \rightarrow XeO(^1\Sigma^+) + O(^3P) \quad 13.1 \text{ kcal/mol}$$

From the mass spectrometric study of Ref. [11] we have D(O–XeO$_2$) = 62 ± 2.6 kcal/mol and D(O–XeO$_3$) = 22.1 ± 2.4 kcal/mol, but it is not clear in this paper what is the electronic state of the outcoming fragments.

All geometrical parameters and harmonic frequencies given in Table 1 are in good agreement with the existing experimental data. As to the dipole moments, there are no experimental values for any

Table 2
Energies E (E_h), geometrical parameters (Å, deg), binding energies D_0 (kcal/mol), atomization energies ΔH_{atom} (kcal/mol), dipole moments μ (D), net Mulliken charges q (e), and harmonic frequencies ω_e (cm^{-1}) of the lowest closed singlet state of XeS_n, n = 1–4.[a]

Species	$-E$	r(Xe–S)	∠S–Xe–S	D_0[b]	ΔH_{atom}[c]	μ	q_{Xe}	ω_e
$XeS(^1\Sigma^+)$	726.150159	2.451	–	12.7	−13.4	3.5	+0.51	275
$XeS_2(^1A_1)$	1123.809344	2.363	119.9	30.3	−21.4	2.7	+1.11	a_1 91, a_1 293, b_2 324
$XeS_3(^1A_1)$	1521.477573	2.310	110.1	53.1	−37.8	1.8	+1.68	e 114, a_1 137, a_1 328, e 361
$XeS_4(^1A_1)$	628.624297	2.260	109.47	74.4	−29.08	0.0	+2.26	e 112, t_2 147, a_1 326, t_2 369

[a] Net Mulliken charges are from HF calculations, harmonic frequencies are obtained at the RCCSD(T)/aug-cc-pVTZ level. All other numbers are at the RCCSD(T)/aug-cc-pV5Z level.
[b] With respect to $Xe(^1S) + nS(^1D)$.
[c] With respect to $Xe(^1S) + nS(^3P)$.

of the species studied here. For the polar XeO_2 and XeO_3 we have computed μ = 3.9 and 3.5 D, respectively.

3.2. Sulfides

Table 2 collects our results on XeS_n, n = 1, 2, 3, 4. As a first remark, we see that in all cases the corresponding atomization energies are negative. However, all geometries reported in Table 2 are local minima with real harmonic frequencies. The intrinsic binding energies D_0, with respect to $Xe(^1S) + nS(^1D)$, are approximately one third of the corresponding XeO_n D_0's. Of course the binding mode must be the same as in the case of oxides, Schemes 1 and 2. However the electron transfer $Xe(^1S) \rightarrow S(^1D)$ is not so efficient as S is less electronegative than O. This is confirmed by the smaller net Mulliken charges and, also, dipole moments, as compared to XeO_n.

Fig. 2 presents RCCSD(T) PEC's of the lowest $^3\Pi$, $^3\Sigma^-$, and $^1\Sigma^+$ states of XeS. As in XeO, we also performed MRCI calculations and the corresponding MRCI + Q PEC's are given as an inset of the same figure. We can see that they are almost identical to the RCCSD(T) ones stressing the appropriateness of the RCCSD(T) methodology.

The two lowest triplets are repulsive with van der Waals minima at 3.954 Å ($^3\Pi$, D_e = 237 cm^{-1}) and 4.543 Å ($^3\Sigma^-$, D_e = 124 cm^{-1}). They cross the first bound state $^1\Sigma^+$ at r(Xe–S) = 2.651 Å ($^3\Pi$) and 2.909 Å ($^3\Sigma^-$). The RCCSD(T) [MRCI + Q] values r_e = 2.451 [2.453] Å and D_0 = 12.7 [12.3] kcal/mol obtained for the $1^1\Sigma^+$ state are again in disagreement with r_e = 2.62 Å and D_e = 7.6 - kcal/mol proposed by Yamanishi et al. [23].

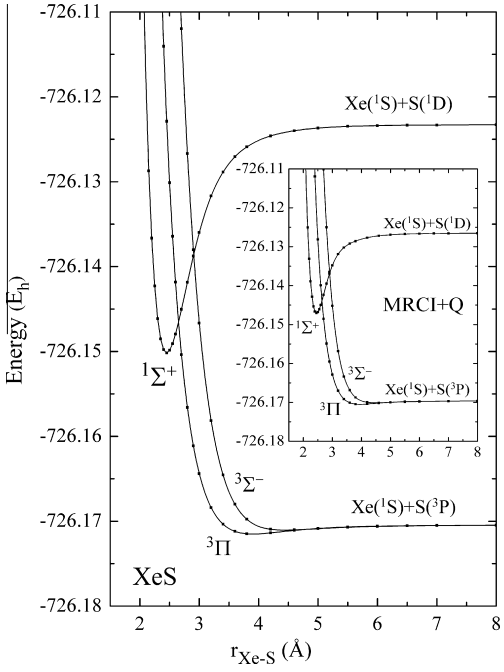

Fig. 2. Potential energy curves of the low-lying $^3\Pi$, $^3\Sigma^-$, and $^1\Sigma^+$ electronic states of XeS at the RCCSD(T)/aug-cc-pV5Z and MRCI + Q/aug-cc-pV5Z (inset) levels of theory.

For the same state the following spectroscopic constants were calculated: ω_e = 275 cm^{-1}, $\omega_e x_e$ = 2.3 cm^{-1}, $a_e = 0.9 \times 10^{-3}$ cm^{-1}, and $\bar{D}_e = 6.8 \times 10^{-8}$ cm^{-1}.

Turning to the polyatomic XeS_n, n = 2, 3, 4, we observe again a monotonic increase of the mean Xe–S binding energy followed by a concomitant decrease of bondlengths as the number of S atoms increases.

Experimental data are not available for xenon polysulfides. Theoretical MP2 calculations on XeS_3, by Ball [25], yielded r(Xe–S) = 2.393 Å, ∠S–Xe–S = 110.8°, and μ = 2.32 D. Our corresponding numbers r(Xe–S) = 2.310 Å, ∠S–Xe–S = 110.1°, and μ = 1.85 D are judged more reliable.

Concluding this section, we quote, below, some numbers concerning the intrinsic Xe–S bond strengths, calculated at the RCCSD(T)/aug-cc-pV5Z level:

$$XeS_4(^1A_1) \rightarrow XeS_3(^1A_1) + S(^1D) \quad 21.2 \text{ kcal/mol}$$

$$XeS_3(^1A_1) \rightarrow XeS_2(^1A_1) + S(^1D) \quad 22.8 \text{ kcal/mol}$$

$$XeS_2(^1A_1) \rightarrow XeS(^1\sigma^+) + S(^1D) \quad 17.5 \text{ kcal/mol}$$

These findings dictate that it would be possible to trap some of the above species at low temperatures, e.g. on cryogenic matrices, since they occupy well defined local minima on the $Xe(^1S) + nS(^1D)$ hypersurface. Of course this depends, also, on the topology of the surfaces stemming from lower asymptotic channels.

3.3. Oxysulfides

Replacement of one or more oxygen atoms in xenon oxides, with sulfur, results in the different xenon oxysulfide systems, XeO_nS_m. Again, bonding is expected to occur through the mechanism of Scheme 2. All our findings are presented in Table 3. The corresponding molecular symmetries are C_s (XeOS, XeO_2S, and $XeOS_2$), C_{2v} (XeO_2S_2), and C_{3v} ($XeOS_3$ and XeO_3S). In all cases the geometries reported in Table 3 represent real local minima on the corresponding potential energy surfaces.

As we can see all species are bound with respect to the $Xe(^1S) + nO(^1D) + mS(^1D)$ atomic fragments, while XeO_2S, XeO_2S_2, and XeO_3S are, also, bound with respect to the ground state $Xe(^1S) + nO(^3P) + mS(^3P)$ atomic channel by 18.2, 19.7, and 49.3 kcal/mol, respectively. The latter three systems are analogous to XeO_4 (XeO_3S and XeO_2S_2) and to XeO_3 (XeO_2S) which are isolable. Thus, it is reasonable to check how tightly the S atoms are connected to Xe, in order to get some insight about their stability. Below, are given numerical results at the RCCSD(T)/aug-cc-pV5Z level including ZPE corrections:

$$XeO_3S(^1A_1) \rightarrow XeO_3(^1A_1) + S(^3P) \quad 4.6 \text{ kcal/mol}$$

Table 3
Energies E (E_h), geometrical parameters (Å, deg), binding energies D_0 (kcal/mol), ΔH_{at} atomization energies (kcal/mol), dipole moments μ (D), net Mulliken charges q (e), and harmonic frequencies ω_e (cm^{-1}) of the lowest closed singlet state of XeO_nS_m.[a]

Species	$-E$	r(Xe–O) r(Xe–S)	∠O–Xe–S ∠O–Xe–O ∠S–Xe–S	D_0[b]	ΔH_{atom}[c]	μ	q_{Xe} q_O q_S	ω_e
XeOS ($^1A'$)	801.155468	1.868 2.310	116.2 – –	59.7	−11.3	3.3	+1.54 −0.94 −0.60	a′ 142, a′ 360, a′ 643
XeO_2S ($^1A'$)	876.206331	1.796 2.238	108.8 106.2 –	134.4	18.2	3.2	+2.66 −1.03 −0.60	a″ 182, a′ 223, a′ 256, a′ 427, a′ 745, a″ 799
$XeOS_2$ ($^1A'$)	1198.839244	1.820 2.262	108.3 – 111.0	92.1	−4.8	2.8	+2.20 −1.00 −0.60	a′ 129, a″ 187, a′ 192, a′ 382, a″ 398, a′ 717
XeO_2S_2 ($^1A_1$)	1273.881851	1.779 2.230	109.2 106.3 113.3	161.7	19.7	2.1	+3.14 −1.04 −0.54	a_1 134, a_2 183, b_2 188, b_1 254, a_1 267, a_1 391, b_1 414, a_1 770, b_2 822
XeO_3S ($^1A_1$)	951.259609	1.780 2.241	111.1 107.8 –	216.5	49.3	2.5	+3.49 −1.00 −0.49	e 185, e 271, a_1 293, a_1 414, a_1 775, e 850
$XeOS_3$ ($^1A_1$)	1596.504660	1.810 2.274	107.7 – 111.2	113.1	−9.6	1.6	+2.55 −0.99 −0.52	e 128, a_1 154, e 218, a_1 362, e 395, a_1 761

[a] Net Mulliken charges are from HF calculations, harmonic frequencies are obtained at the RCCSD(T)/aug-cc-pVTZ level. All other numbers are at the RCCSD(T)/aug-cc-pV5Z level.
[b] With respect to Xe(^1S) + nO(^1D) + mS(^1D).
[c] With respect to Xe(^1S) + nO(^3P) + mS(^3P).

$$XeO_2S_2(^1A_1) \rightarrow XeO_2S(^1A') + S(^3P) \quad 1.4\ \text{kcal/mol}$$

$$XeO_2S(^1A') \rightarrow XeO_2(^1A_1) + S(^3P) \quad 16.4\ \text{kcal/mol}$$

The first two numbers indicate that removal of an S(^3P) atom from XeO_3S and XeO_2S_2 can proceed very easily. Consequently, these two systems are not expected to be stable. However, in XeO_2S the Xe–S binding energy raises to 16.4 kcal/mol. In the same system the Xe–O binding energy, with respect to XeOS($^1A_1$) + O(^3P), was found 29.5 kcal/mol. The atomization energy of XeO_2S is slightly less than half the atomization energy of XeO_3, Tables 1 and 2.

In view of the above results, we believe that XeO_2S might be isolated under proper conditions, albeit, with more difficulty than XeO_3.

Concluding this section we must mention that, to our knowledge, no experimental work exists in the literature on xenon oxysulfides, while the only theoretical paper by Ball [25] reports calculations, at various levels of theory, on XeO_2S and $XeOS_2$. Our calculated geometries and harmonic frequencies, Table 3, compare relatively well with Ball's numbers at the MP2 level. This author suggests, at the same level, as upper limits of heats of formation ΔH_f[XeO_2S] = 210.6 kcal/mol and ΔH_f[$XeOS_2$] = 260.3 kcal/mol. Using as atomic heats of formation our calculated ΔH_f[O(g)] = 58.3 kcal/mol and the experimental [32] ΔH_f[S(g)] = 65.7 kcal/mol, we obtain ΔH_f[XeO_2S(g)] = 164.1 kcal/mol and ΔH_f[$XeOS_2$(g)] = 194.5 kcal/mol, much lower than Ball's corresponding values.

4. Synopsis and conclusions

We studied theoretically all possible closed-shell xenon oxides, sulfides, and oxysulfides using the RCCSD(T) methodology in conjunction with basis sets of augmented quintuple-ζ quality. For all species we determined geometrical parameters, binding and atomization energies, dipole moments, and harmonic frequencies. Some major conclusions and results are summarized below.

In all XeO_nS_m systems, the in situ electronic configuration of the O and/or S atoms corresponds to their first excited ^1D state. The bonding mechanism implies a Xe → O or S electron transfer. The Xe–O and Xe–S bonds bear ionic character which is more pronounced in the case of the former. All species are bound with respect to the Xe(^1S) + nO(^1D) + mS(^1D) atomic channel with D_0 values ranging from ∼13 kcal/mol (XeS) to ∼250 kcal/mol (XeO_4).

Xenon oxides XeO_n, with n = 2, 3, 4, are bound with respect to Xe(^1S) + nO(^3P) with atomization energies 1.9, 44.7, and 70.7 kcal/mol, respectively. These values yield the following heats of formation (at 0° K): ΔH_f[XeO_2(g)] = 114.7 kcal/mol, ΔH_f[XeO_3(g)] = 130.2 kcal/mol, and ΔH_f[XeO_4(g)] = 162.5 kcal/mol. To our knowledge these are the most accurate theoretical results so far.

All xenon sulfides have negative atomization energies. The calculated heats of formation, using the experimental ΔH_f[S(g)] (vide supra), are (in kcal/mol) ΔH_f[XeS(g)] = 79.1, ΔH_f[XeS_2(g)] = 152.8, ΔH_f[XeS_3(g)] = 234.9, and ΔH_f[XeS_4(g)] = 291.9.

Among all six xenon oxysulfide systems studied, XeO_3S, XeO_2S_2, and XeO_2S were found to have positive atomization energies but XeO_2S and XeO_2S_2 can easily lose an S(^3P) atom yielding XeO_3 and XeO_2S, respectively. Finally, XeO_2S is believed, on the basis of our numerical results, to be isolable like its counterpart XeO_3, albeit under more stringent conditions.

References

[1] C.L. Chernick, H.H. Claassen, P.R. Fields, H.H. Hyman, J.G. Malm, W.M. Manning, M.S. Matheson, L.A. Quarterman, F. Schreiner, H.H. Selig, I. Sheft, S. Siegel, E.N. Sloth, L. Stein, M.H. Studier, J.L. Weeks, M.H. Zirin, Fluorine compounds of Xenon and Radon, Science 138 (1962) 136–138.
[2] J.L. Weeks, C.L. Chernick, M.S. Matheson, Photochemical preparation of Xenon difluoride, J. Am. Chem. Soc. 84 (1962) 4612–4613.
[3] N. Bartlett, Xenon hexafluoroplatinate (V) Xe + $[PtF6]^-$, Proc. Chem. Soc. 1962, pp. 218–218.
[4] D.F. Smith, Xenon oxyfluoride, Science 140 (1963) 899–900.
[5] D.F. Smith, Xenon trioxide, J. Am. Chem. Soc. 85 (1963) 816–817.
[6] J.L. Huston, M.H. Studier, E.N. Sloth, Xenon tetroxide: mass spectrum, Science 143 (1964) 1161–1162.
[7] H. Selig, H.H. Claassen, C.L. Chernick, J.G. Malm, J.L. Huston, Xenon tetroxide: preparation and some properties, Science 143 (1964) 1322–1323.
[8] D.H. Templeton, A. Zalkin, J.D. Forester, S.M. Williamson, Crystal and molecular structure of xenon trioxide, J. Am. Chem. Soc. 85 (1963) 817.
[9] G. Gundersen, K. Hedberg, J.L. Huston, Molecular structure of xenon tetroxide, XeO_4, J. Chem. Phys. 52 (1970) 812–815.
[10] H.H. Claassen, G. Knapp, Raman spectrum of xenic acid, J. Am. Chem. Soc. 86 (1964) 2341–2342.

[11] J.L. Huston, H.H. Claassen, Raman spectra and force constants for OsO_4 and XeO_4, J. Chem. Phys. 52 (1970) 5646–5648.
[12] R.S. McDowell, L.B. Asprey, Vibrational spectrum and force field of xenon tetroxide, J. Chem. Phys. 57 (1972) 3062–3068.
[13] S. R. Gunn, Noble gas compounds 149, in: H. H. Hyman (Ed.), University of Chicago Press, Chicago Il, 1963.
[14] S.R. Gunn, The heat of formation of xenon tetroxide, J. Am. Chem. Soc. 87 (1965) 2290–2291. and references therein.
[15] V.V. Zelenov, E.V. Aparina, A.V. Loboda, A.S. Kukui, A.F. Dodonov, S.A. Kastanov, N.N. Aleinikov, Mass spectrometric studies of physical, thermochemical and reactive properties of xenon fluorides, xenon oxides and xenon oxyfluorides, Eur. J. Mass Spectrom. 8 (2002) 233–246.
[16] N. Bartlett, P.K. Rao, Xenon hydroxide: an experimental hazard, Science 139 (1963) 506.
[17] D.S. Brock, G.J. Schrobilgen, Synthesis of the missing oxide XeO_2, and its implications for Earth's missing xenon, J. Am. Chem. Soc. 133 (2011) 6265–6269.
[18] C.D. Cooper, M. Lichtenstein, Spectra of argon, oxygen, and nitrogen mixtures, Phys. Rev. 109 (1958) 2026–2028.
[19] C.D. Cooper, G.C. Cobb, Visible spectra of XeO and KrO, in: E.I. Tolnas, J. Mol. Spectrosc. vol. 7, 1961, pp. 223–230.
[20] J. Xu, D.W. Setser, J.K. Ku, Xenon oxide and xenon sulfide emission systems at 234 and 227 nm, Chem. Phys. Lett. 132 (1986) 427–435.
[21] T.H. Dunning, P.J. Hay, Low-lying electronic states of the rare gas oxides, J. Chem. Phys. 66 (1977) 3767–3777.
[22] S.R. Langhoff, Theoretical treatment of the spin–orbit coupling in the rare gas oxides NeO, ArO, KrO, and XeO, J. Chem. Phys. 73 (1980) 2379–2386.
[23] M. Yamanichi, K. Hirao, K. Yamachita, Theoretical study of the low-lying electronic states of XeO and XeS, J. Chem. Phys. 108 (1998) 1514–1521.
[24] P. Pyykkö, T. Tamm, Calculations for XeO_n (n = 2–4): could the xenon dioxide molecule exist?, J Phys. Chem. A 104 (2000) 3826–3828.
[25] D.W. Ball, On the stability of xenon oxysulfides and sulfides, J. Mol. Struct. (Theochem) 532 (2000) 239–244.
[26] R.V. Taylor, W.C. Walker, Photoluminescence of ArS, KrS, and XeS in rare gas matrices, Appl. Phys. Lett. 35 (1979) 359–360.
[27] K.A. Peterson, D. Figgen, E. Goll, H. Stoll, M. Dolg, Systematically convergent basis sets with relativistic pseudopotentials. II. Small-core pseudopotentials and correlation consistent basis sets for the post-d group 16–18 elements, J. Chem. Phys. 119 (2003) 11113–11123.
[28] T.H. Dunning Jr., Gaussian basis sets for use in correlated molecular calculations. I. The atoms boron through neon and hydrogen, J. Chem. Phys. 90 (1989) 1007–1023.
[29] D.E. Woon, T.H. Dunning Jr., Gaussian basis sets for use in correlated molecular calculations. III. The atoms aluminum through argon, J. Chem. Phys. 98 (1993) 1358–1371.
[30] C.E. Moore, Atomic Energy Levels, NSRDS-NBS Circular No 35, US GPO, Washington DC, 1971.
[31] MOLPRO, version 2010.1, a package of ab initio programs, H.-J. Werner, P.J. Knowles, R. Lindh, F. R. Manby, M. Schütz, P. Celani, T. Korona, A. Mitrushenkov, G. Rauhut, T. B. Adler, R. D. Amos, A. Bernhardsson, A. Berning, D. L. Cooper, M. J. O. Deegan, A. J. Dobbyn, F. Eckert, E. Goll, C. Hampel, G. Hetzer, T. Hrenar, G. Knizia, C. Köppl, Y. Liu, A. W. Lloyd, R. A. Mata, A. J. May, S. J. McNicholas, W. Meyer, M. E. Mura, A. Nicklass, P. Palmieri, K. Pflüger, R. Pitzer, M. Reiher, U. Schumann, H. Stoll, A. J. Stone, R. Tarroni, T. Thorsteinsson, M. Wang, A. Wolf, see <http://www.molpro.ne>.
[32] NIST Standard Reference Database 13. NIST JANAF THERMOCHEMICAL TABLES, 1985, Version 1.0. <http://kinetics.nist.gov/janaf>.